Supplemental Materials

Molecular Biology of the Cell

Irianto et al.

Fig. S1. GFP-53BP1 do not occupy nucleolus regions and YFP-NLS also segregates in small 3 μm constrictions

(A) U2OS cells were co-transfected with GFP-53BP1 and mApple-Fibrillarin, which indicates the presence of nucleoli. The representative image clearly show the exclusion of GFP-53BP1 and Hoechst stained DNA from the nucleoli.

(B) Representative images showing the segregation of YFP-NLS-MS2 inside the 3 μm pore.

Fig. S2. Acetylated histone H3 follows DNA behavior in constrictions.

(A,B) Following DNA behavior, the level of acetylated histone H3 (acetyl-H3) is enriched within the 3 μm pore constrictions, hence the intensity ratio is above one (≥ 15 cells; n = 2 expts). However, the enrichment of acetyl-H3 is not as high as the DNA, probing the need to test acetyl-H3 antibody specificity. **(C)** Indeed, inhibition of histone deacetylase by 300 nM Trichostatin A for 12 hours resulted in an increase in acetyl-H3 level, as shown by the antibody immunostaining (≥ 120 cells per group, $*p < 0.05$)

Fig. S3. Mobile protein segregation is an unavoidable physical effect of nuclear constriction.

Well over 90% of aspirated cells exhibit segregation; even those that do not appear to be within statistical uncertainty of doing so (≥4 cells per group; n ≥ 3 expts).

Fig. S4 Nuclear FokI levels are higher with addition of tamoxifen and seem to accumulate over time. Nuclear FokI levels increase with the addition of tamoxifen to the 1 μM Shield1 treated cells. The amount of FokI in the nuclei is higher at 24 hours, when compared to the 6 hours treated cells (≥ 100 cells per group, n ≥ 2 expts, $*p < 0.05$, $**p < 0.01$).

Fig. S5 H2B-GFP at the FokI foci are not depleted over time.

(A) Representative images of the observation of H2B-GFP and mCherry-FokI levels at the FokI focus region, over a period of 20 minutes. Intensity profiles across the FokI foci and the surrounding H2B-GFP show the depletion of FokI at the focus, but not H2B-GFP.

(B,C) Intensity profiles of two different nuclei, also show the depletion of FokI, but not H2B-GFP.

Figure S1

GFP-Ku80 also segregates in small 3 μm constrictions

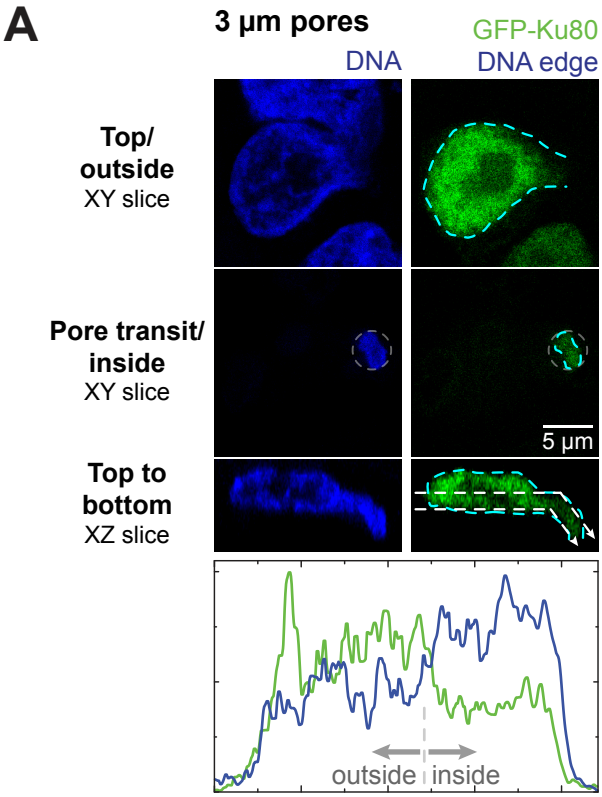

Nuclear GFP-53BP1 proteins are excluded from the nucleoli

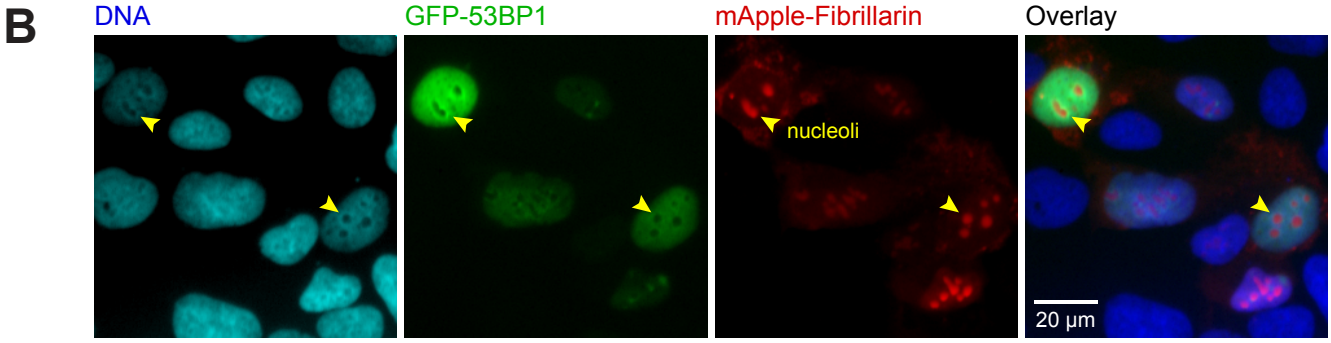

Figure S2

Acetylated histone H3 follows DNA and other chromatin-bound proteins behaviour in constrictions

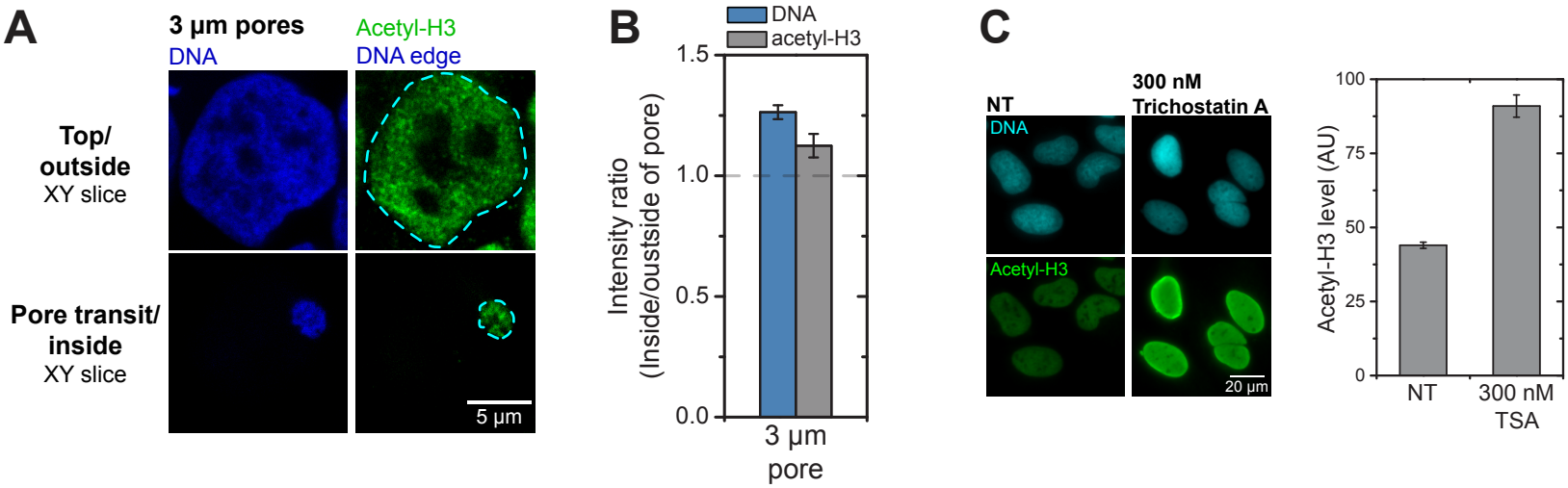

Figure S3

Scatter plot of intensity ratio data shows >90% of (DNA measurement ≥ 1.0) and (mobile factors ≤ 1.0)

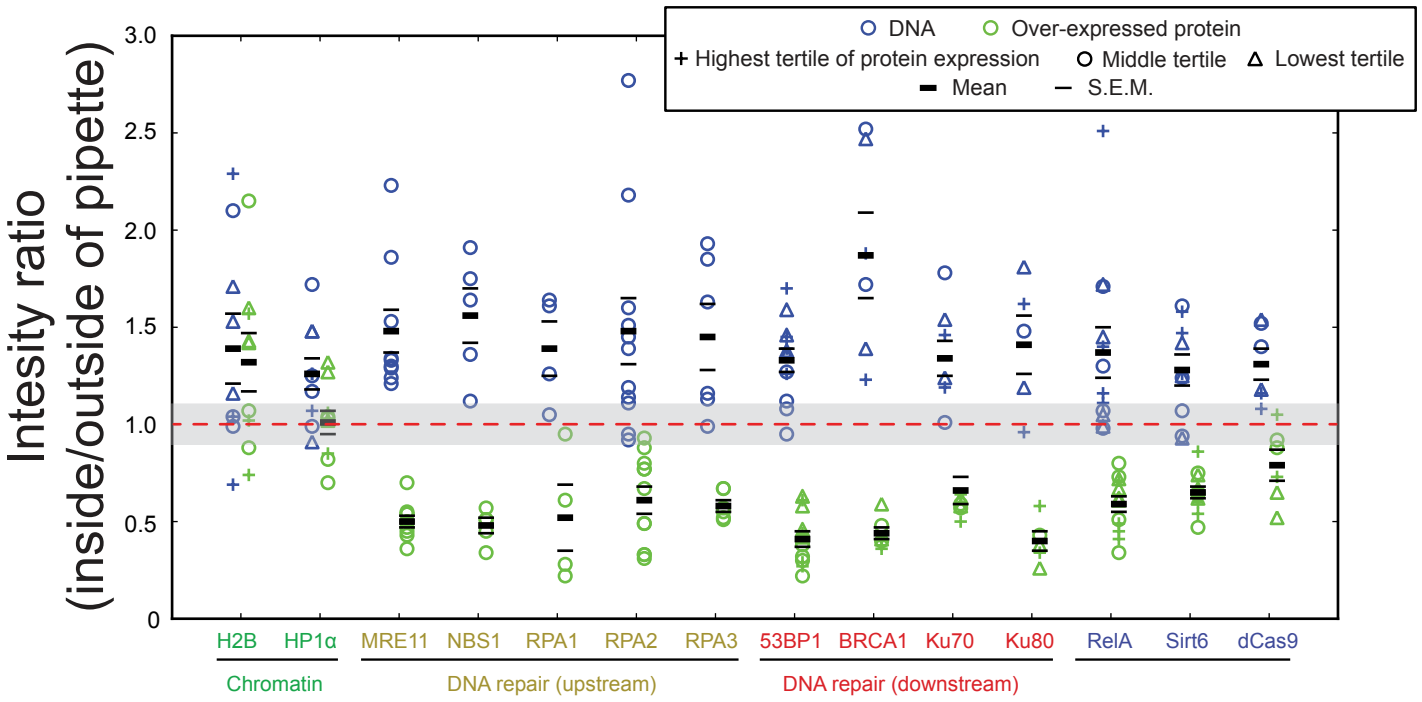

Figure S4

Nuclear FokI levels are higher with addition of Tamoxifen and seem to accumulate over time

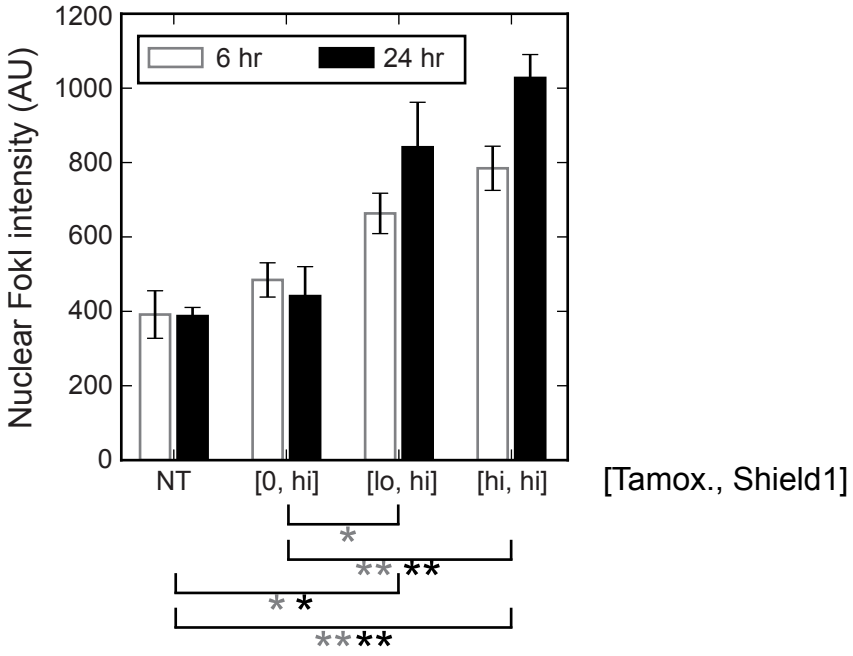

Figure S5

H2B remains in the FokI locus site during aspiration

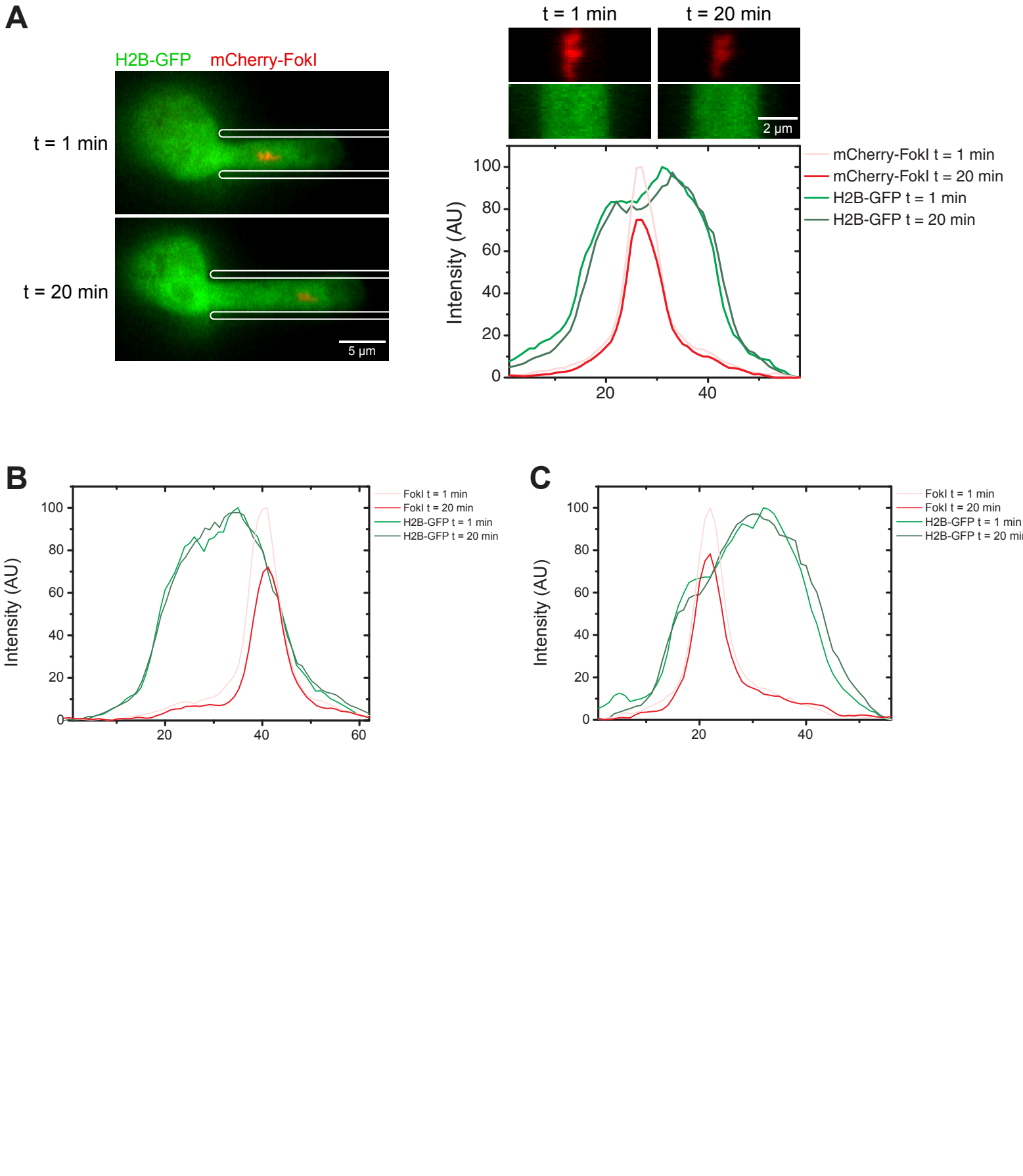

Table S1 FRAP data of non-foci bound nucleoplasmic GFP-tagged protein

GFP-tagged protein	Molecular weight[S1], kDa (+GFP)	Estimated Isoelectric point, pI[S1] (+GFP)	Mobile fraction	recover half-time	recover time
RPA3	14 (41)	4.8 (5.2)			
GFP	27	5.4	95%[S2,3]	1 s	4-7 s
RPA2	29 (56)	5.4 (5.5)			
Sirt6	35 (62)	6.0 (5.7)			
YFP-MS2	42	5.6			
RelA	60 (87)	5.3 (5.4)	95%[S3]	1 s	7 s
RPA1	68 (95)	6.5 (5.8)	95%[S4]	8 s	30 s
Ku70	70 (97)	6.1 (5.8)	90%[S5,6]	6-7 s	20 s
Mre11	81 (108)	5.4 (5.4)	95%[S7]	3 s	30 s
Ku80	82 (109)	5.4 (5.4)	90%[S8]	1 s	3 s
NBS1	85 (112)	6.2 (5.9)	95%[S9,10]	0.5 s	3 s
dCas9	158 (185)	8.2 (7.8)			
MDC1	196 (223)	5.0 (5.1)	95%[S9,10]	2 s	7 s
BRCA1	208 (235)	5.2 (5.2)			
53BP1	214 (241)	4.5 (4.6)	100%[S11]	5 s	50 s

References

S1. Kozlowski, L. P., IPC - Isoelectric Point Calculator. ***bioRxiv***. 2016.

S2. Zheng, C. Y., R. S. Petralia, Y. X. Wang, and B. Kachar, Fluorescence recovery after photobleaching (FRAP) of fluorescence tagged proteins in dendritic spines of cultured hippocampal neurons. ***J Vis Exp***. (50), 2011.

S3. Bosisio, D., I. Marazzi, A. Agresti, N. Shimizu, M. E. Bianchi, and G. Natoli, A hyper-dynamic equilibrium between promoter-bound and nucleoplasmic dimers controls NF-kappaB-dependent gene activity. ***EMBO J***. 25 (4):798-810, 2006.

S4. Gourdin, A. M., L. van Cuijk, M. Tresini, M. S. Luijsterburg, A. L. Nigg, G. Giglia-Mari, A. B. Houtsmuller, W. Vermeulen, and J. A. Marteijn, Differential binding kinetics of replication protein A during replication and the pre- and post-incision steps of nucleotide excision repair. ***DNA Repair (Amst)***. 24:46-56, 2014.

S5. Rodgers, W., S. J. Jordan, and J. D. Capra, Transient association of Ku with nuclear substrates characterized using fluorescence photobleaching. ***J Immunol***. 168 (5):2348-55, 2002.

S6. Byrum, J., S. Jordan, S. T. Safrany, and W. Rodgers, Visualization of inositol phosphate-dependent mobility of Ku: depletion of the DNA-PK cofactor InsP6 inhibits Ku mobility. ***Nucleic Acids Res***. 32 (9):2776-84, 2004.

S7. Boisvert, F. M., M. J. Hendzel, J. Y. Masson, and S. Richard, Methylation of MRE11 regulates its nuclear compartmentalization. ***Cell Cycle***. 4 (7):981-9, 2005.

S8. Mari, P. O., B. I. Florea, S. P. Persengiev, N. S. Verkaik, H. T. Bruggenwirth, M. Modesti, G. Giglia-Mari, K. Bezstarosti, J. A. Demmers, T. M. Luider, A. B. Houtsmuller, and D. C. van Gent, Dynamic assembly of end-joining complexes requires interaction between Ku70/80 and XRCC4. ***Proc Natl Acad Sci U S A***. 103 (49):18597-602, 2006.

S9. Lukas, C., F. Melander, M. Stucki, J. Falck, S. Bekker-Jensen, M. Goldberg, Y. Lerenthal, S. P. Jackson, J. Bartek, and J. Lukas, Mdc1 couples DNA double-strand break recognition by Nbs1 with its H2AX-dependent chromatin retention. ***EMBO J***. 23 (13):2674-83, 2004.

S10. Tobias, F., D. Lob, N. Lengert, M. Durante, B. Drossel, G. Taucher-Scholz, and B. Jakob, Spatiotemporal dynamics of early DNA damage response proteins on complex DNA lesions. ***PLoS One***. 8 (2):e57953, 2013.

S11. Bekker-Jensen, S., C. Lukas, F. Melander, J. Bartek, and J. Lukas, Dynamic assembly and sustained retention of 53BP1 at the sites of DNA damage are controlled by Mdc1/NFBD1. ***J Cell Biol***. 170 (2):201-11, 2005.